SUPPLEMENTARY INFORMATION

Deep Eutectic Solvents as Recyclable Media for Metal Removal from Crude Oil

Eminemi Mirinn,[a] Andrew P. Abbott,[a] and Alexander F. R. Kilpatrick*[a]

[a]School of Chemistry, University of Leicester, University Road, LE1 7RH Leicester, UK.
E-mail: sandy.kilpatrick@leicester.ac.uk

Table of contents

1 Additional characterisation data for copper(II) phthalocyanine green

The molecular structure of copper(II) phthalocyanine green, [Cu(Pc^{Cl16})], is shown in **Figure S1**.

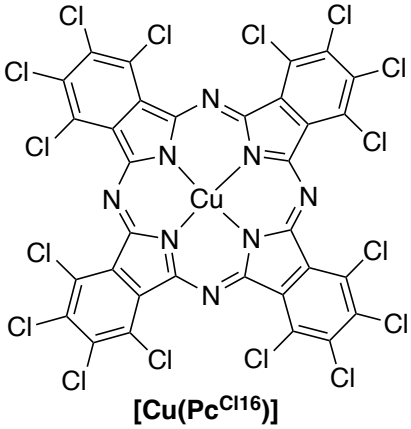

Figure S1 Structure of [Cu(Pc^{Cl16})].

1.1 UV-Vis spectroscopy

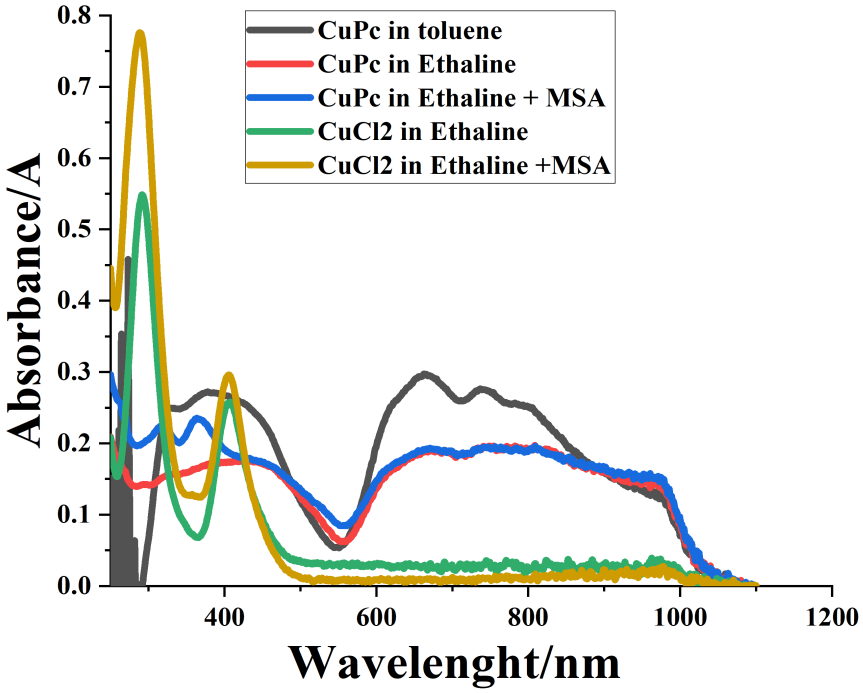

Figure S2 UV-vis spectra of [Cu(Pc^{Cl16})] green in toluene, Ethaline, Ethaline + 10 mmol MSA, and $CuCl_2$ in Ethaline, Ethaline MSA at concentrations of 0.08 mmol dm^{-3}.

It can be seen from **Figure S2** that characteristic two absorption maxima at 400–450 nm and 570–800 nm in the UV-vis absorption spectra are present for [Cu(Pc^{Cl16})]. These are due to the Soret and the Q bands of the copper(II) phthalocyanine green. This is reflected in the Q band transition more pronounced. This corresponds to a transition of electrons from the HOMO to the LUMO.[1] The $CuCl_2 \cdot 2H_2O$ absorbed in the region

of 291–406 nm and these have previously been characterised using EXAFS and are known to be due to $[CuCl_4]^{2-}$.[2]

1.2 Calibration curves

To be able to quantify the extent of solute extraction in DESs previous studies have used liquid-liquid extraction with a variety of solutes.[3] Most of the solutes studied so far have been small organic molecules. It was shown that the more strongly hydrogen bonding solutes partitioned more favourably into the DESs. Previous studies used either GCMS or UV-Vis to quantify the concentration of solutes in the oil and DES phases.[3] In this study the intense colour of [Cu(Pc^{Cl16})] means that UV-Vis is the obvious method to quantify extraction. To be able to quantify concentration of solutes two calibration curves were done at different wavelength using copper phthalocyanine in Ethaline + MSA and toluene at 25 °C in different concentrations and the UV-Vis spectra are shown in **Figure S3**.

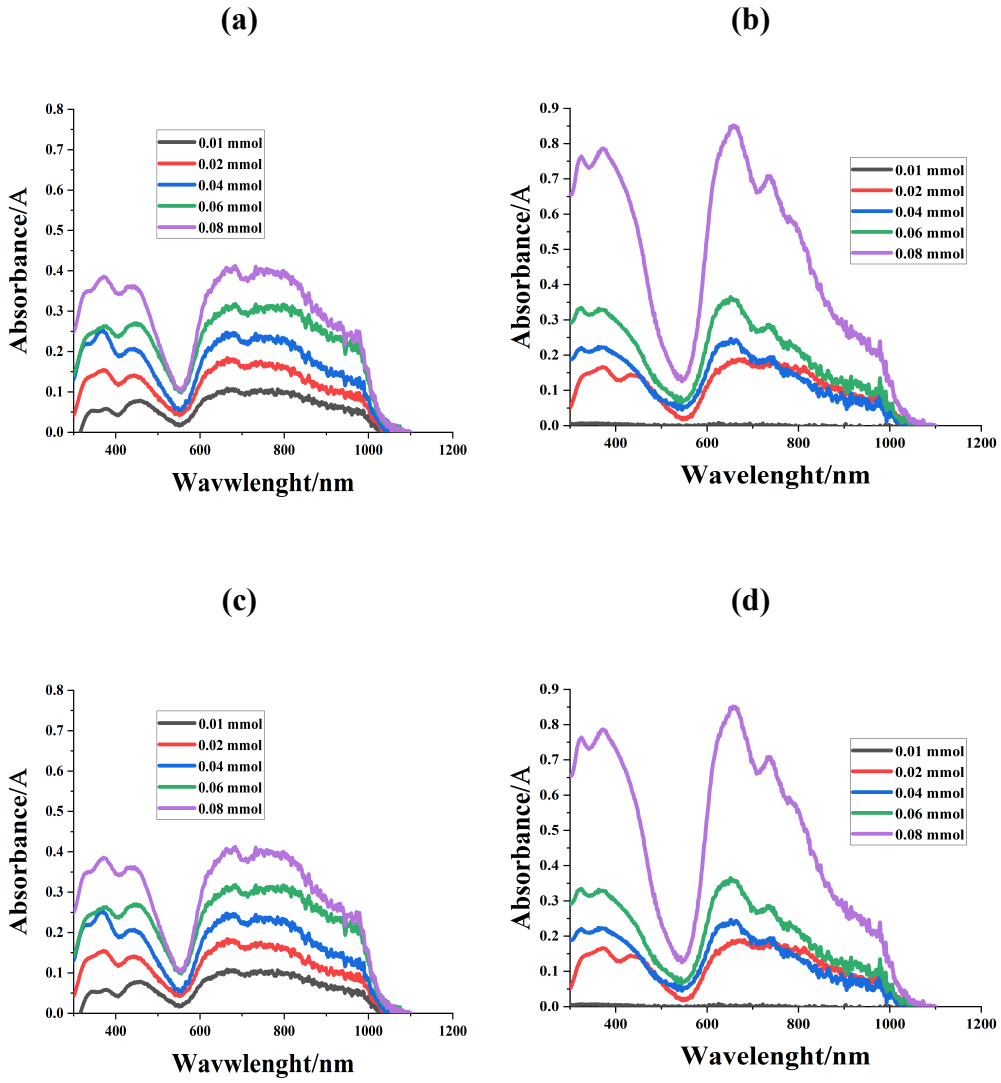

Figure S3 UV-Vis spectra of (a) [Cu(Pc^{Cl16})] in Ethaline + 10 mmol MSA, (b) [Cu(Pc^{Cl16})] in toluene at concentrations of 0.01–0.08 mmol dm^{-3}.

[Cu(Pc^{Cl16})] absorbs over a wide range of wavelengths and the best linear correlation was observed at d→d transitions of Cu centre 450 nm and 650 nm. **Figure S4** shows a linear correlation between absorbance and concentration below 0.08 mmol dm^{-3}. Deviations from linear behaviours were observed above this concentration. It was also noted that the absorbance of [Cu(Pc^{Cl16})] is higher in toluene than in Ethaline + MSA. It can also be seen from the calibration curve that a good linear correlation was obtained with an R^2 value of more than 0.99 for the UV-vis spectroscopy. Due to the smallest uncertainty of the error bars of the values measured, the error bars for almost all the data are within the size of the plot symbols.

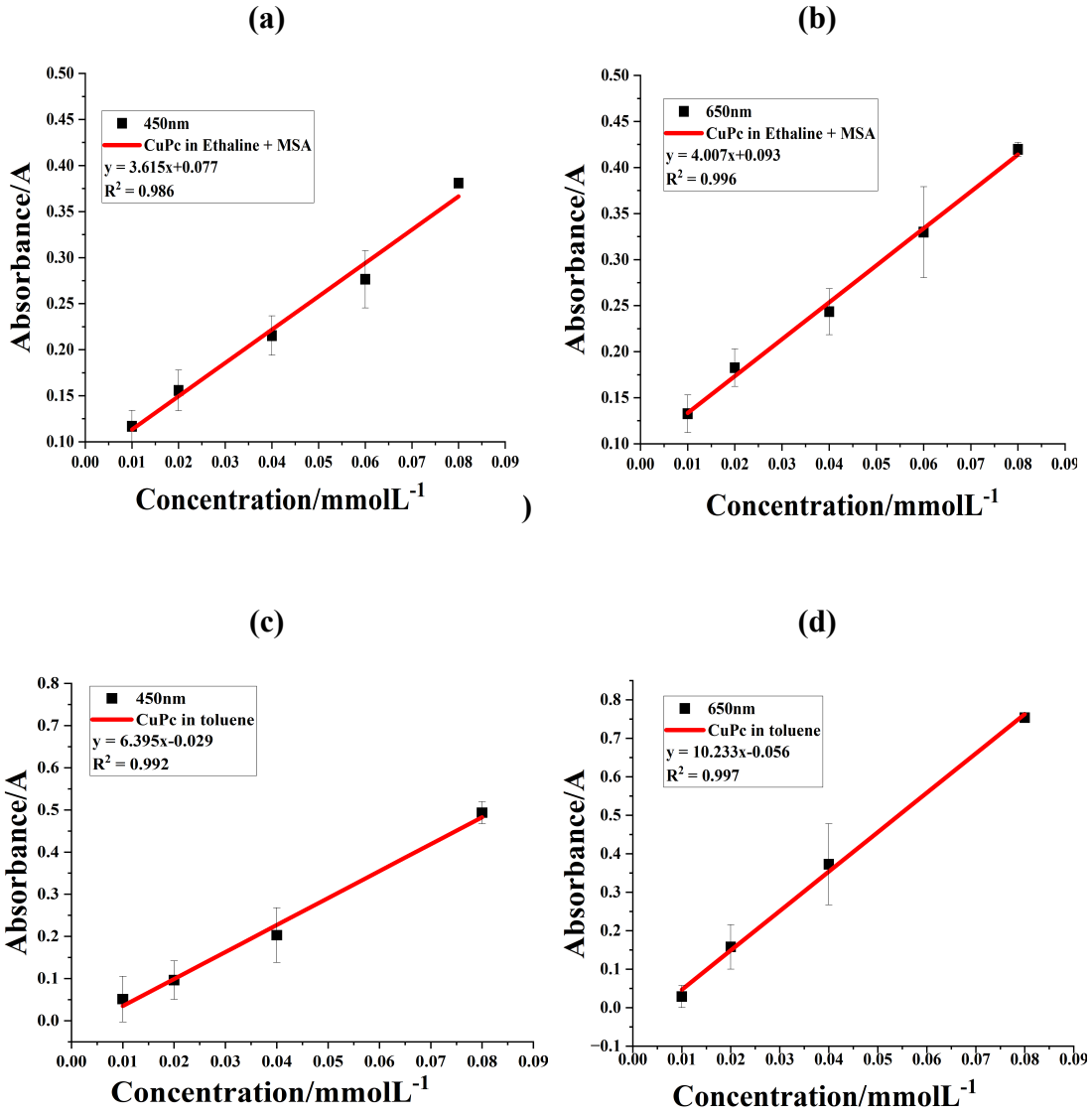

Figure S4 Calibration curve using known standards of [Cu(Pc^{Cl16})] concentration in Ethaline + MSA and toluene at 25 °C with different wavelenghts plotted against (a) 450 nm; (b) 650 nm; (c) 450 nm; (d) 650 nm.

2 Additional characterisation data for iron(II) and nickel(II) phthalocyanato complexes and free-base phthalocyanine

The molecular structures of [Fe(Pc)], [Ni(Pc)] and free-base phthalocyanine H_2Pc are shown in Figure S5.

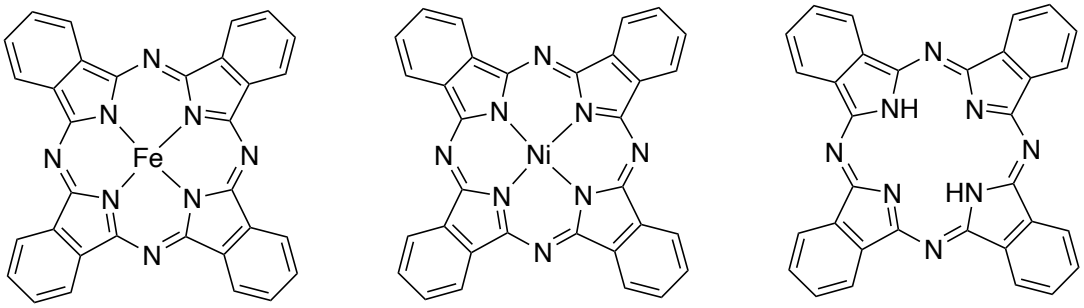

Figure S5 Structures of [Fe(Pc)], [Ni(Pc)] and H_2Pc.

2.1 Calibration curves

UV-vis spectrometry was used for analysis to determine the extent of solute extraction. Calibration curves were prepared to determine the concentration of the solutes at a wavelength of 700 nm for [Fe(Pc)], 707 nm for [Ni(Pc)] and 650 nm for H_2Pc, respectively, using the above-mentioned metallophthalocyanines in toluene at 25 °C in different concentrations. The UV-Vis spectra are shown in **Figure S6**.

The characteristic spectra feature of the phthalocyanine is a result of a conjugated π-electron aromatic cyclic model, which consists of 18- electrons. Analysis of the absorption spectra in the UV region shows a peak which is called the Soret band. This wide absorption band in the UV region is assumed to be UV absorption band edge of molecules of the phthalocyanine. Another known band possessed by the phthalocyanine molecule is the Q-band (visible region) which shows between the 600 nm and 800 nm. As seen in **Figure S6**, the clear peak of [Fe(Pc)], [Ni(Pc)] and H_2Pc observed in the visible region that is the Q-band, has been assumed to be as a result of the π-π* excitation which takes place between the bonding and anti-bonding molecular orbitals.[4]
This work observed a single peak in the Soret band and this is very close to work reported previously for [Co(Pc)].[5] This simply tells us that there is an orbital overlapping of the phthalocyanine ring with the central metal and this affects the structure of the peak when it comes to splitting.

There is an indication of the presence of a *d*-band as a result of the central metal atom. This may be connected to the strong N-peak observed in the Soret region which may be as a result of molecular transition. It is assumed that π-d transition is also taking place here. This is because [Fe(Pc)] and [Ni(Pc)] possess partially occupied *d*-bands which is also observed for [Co(Pc)].[6] The metallophthalocyanines and the free-base phthalocyanine absorbs over a wide range of wavelength and linear correlation was observed at 700 nm, 707 nm, and 650 nm respectively. **Figure S6** shows a linear correlation between absorbance and concentration below 0.10 mmol dm^{-3}. A good linear correlation was obtained showing a R^2 value of more than 0.99 in the UV-Vis spectroscopy. Due to the smallest uncertainty of the error bars of the values measured, as seen

in the calibration curves in **Figure S7** below the error bars for almost all the data are within the size of the plot symbols. This point to the fact that replicate results are accurate.

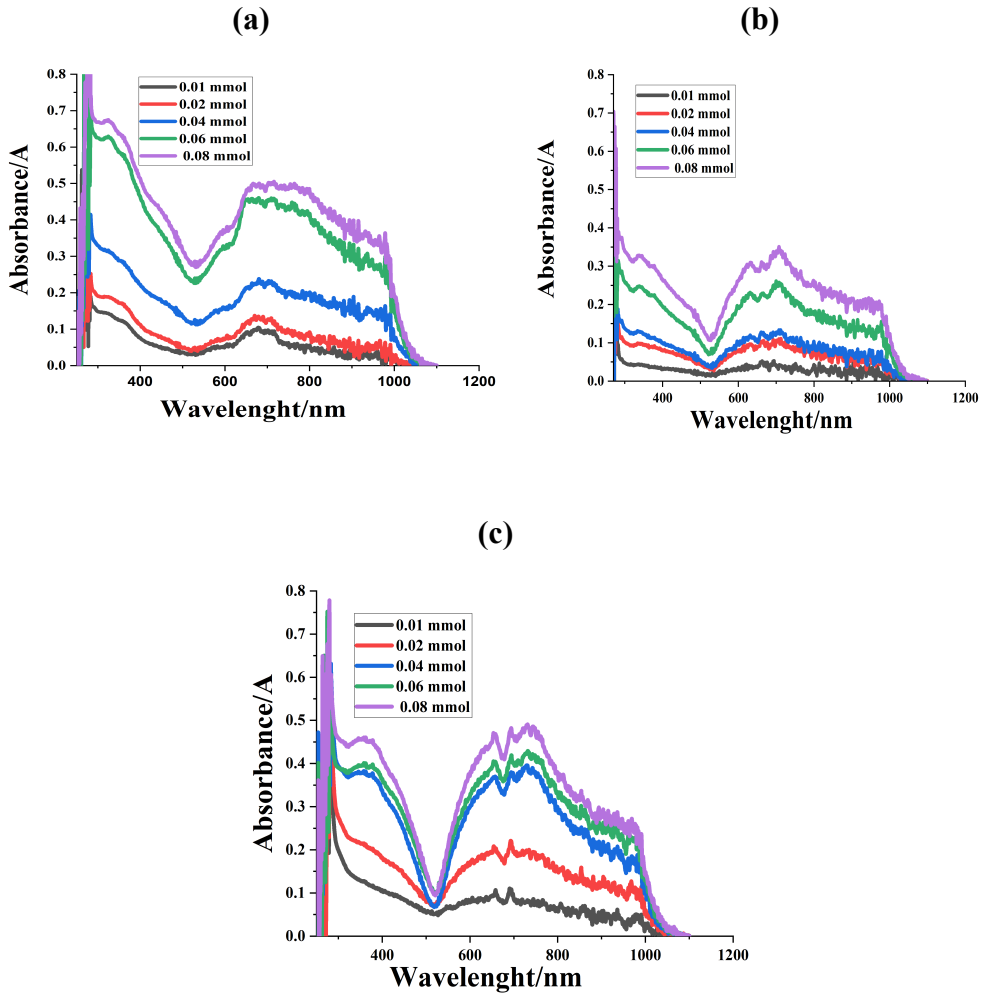

Figure S6 UV-vis spectra of (a) [Fe(Pc)], (b) [Ni(Pc)] (c) H_2Pc in toluene at concentrations of 0.01–0.08 mmol dm^{-3}.

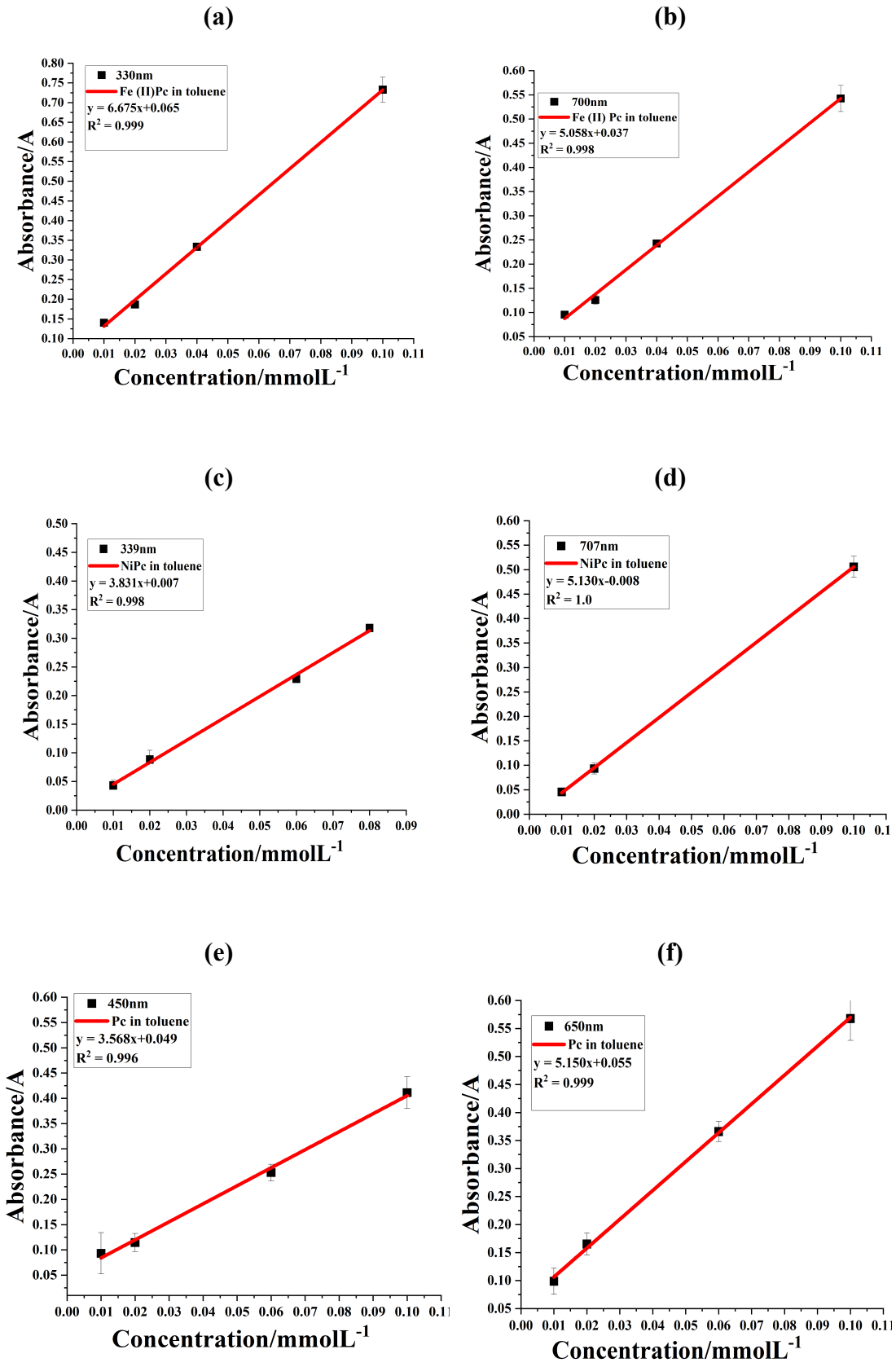

Figure S7 Calibration curves using known standards of (a) [Fe(Pc)], (b) [Ni(Pc)], and (c) H_2Pc concentrations in toluene with different wavelengths plotted against absorbance peaks in UV-Vis spectroscopy.

2.2 Dynamic light scattering (DLS)

Figure S8 below shows particle size curves of [Fe(Pc)], [Ni(Pc)], and H_2Pc in Ethaline and BTMAC:EG +MSA after extraction using the Dynamic Light Scattering technique analysis.

Evaluating homogeneity of the solution from the curves below, although there are major peaks for each measurement, multiple peaks can easily be observed between 100 nm and 4500 nm measuring the radius distribution by intensity for the different solutions. Two peaks at 262±31 nm and 312±64 nm was observed for H_2Pc in Ethaline while three peaks of 940±10 nm, 4240±34 nm, and 1219±67 nm were visible for the H_2Pc in BTMAC:EG +MSA. For [Fe(Pc)], two peaks where visible at 1929±48 nm and 2649 ±202 nm while two peaks were also observed at 1998±71 nm and 2643±291 nm for [Ni(Pc)] in Ethaline.

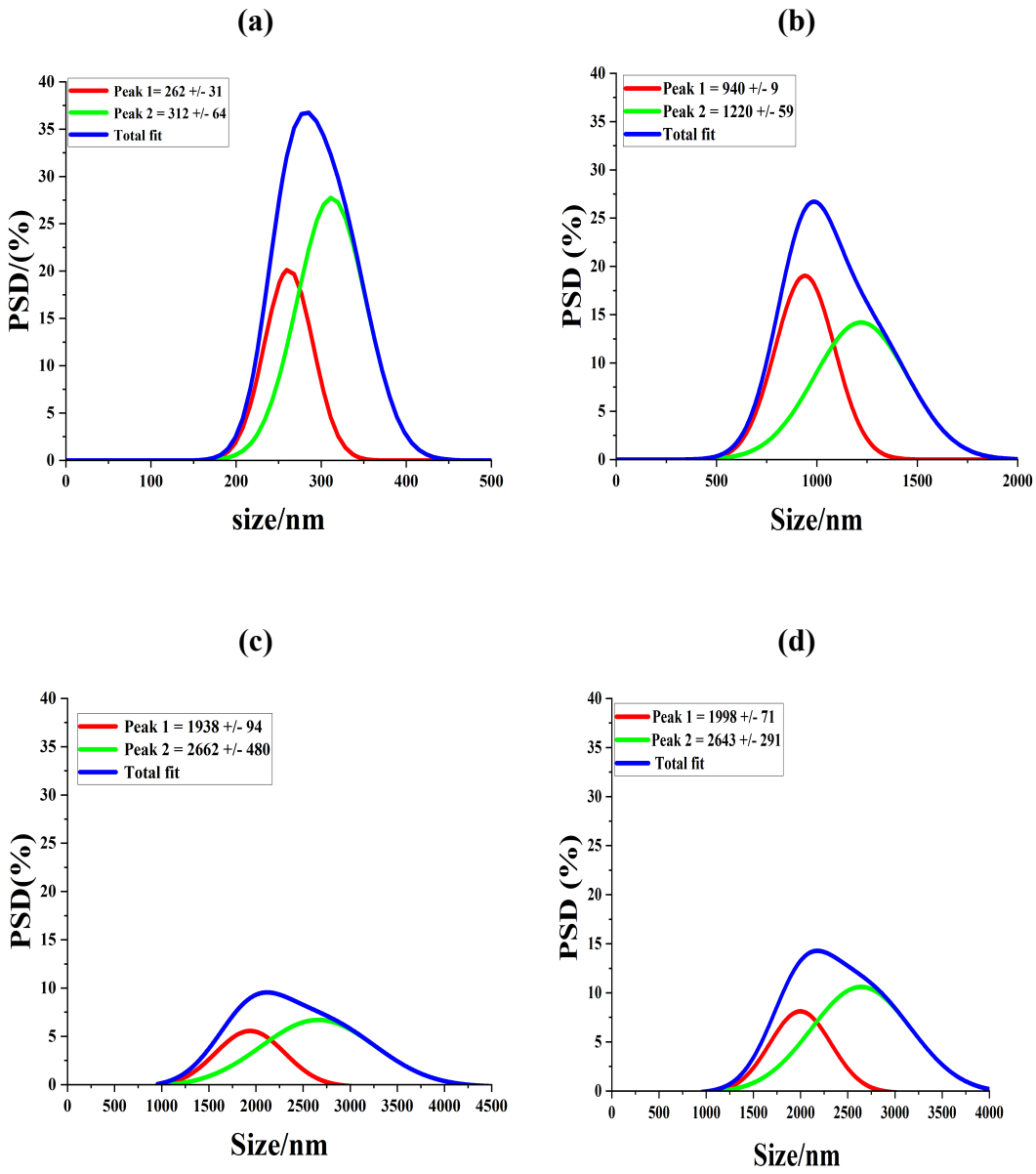

Figure S8 Intensity weighted particle size distributions for 0.0mmol dm^{-3} of (a) H_2Pc in Ethaline after extraction; (b) Pc in BTMAC :EG +MSA; (c) [Fe(Pc)] in Ethaline after extraction; (d) [Ni(Pc)] in Ethaline after extraction.

2.3 Thermodynamics of extraction

The thermodynamic parameters for the extraction of the metallophthalocyanine by the DESs can be determined by measuring the apparent partition coefficients at various temperatures. The changes in Gibbs energy ($\Delta G°$), entropy ($\Delta S°$) and enthalpy ($\Delta H°$) can be determined using Equations S1–S3.

$$\Delta G° = -RTInK_p \quad \text{(S1)}$$

$$ln\left(\frac{K_2}{K_1}\right) = -\frac{\Delta H°}{R}\left(\frac{1}{T_2} - \frac{1}{T_1}\right) \quad \text{(S2)}$$

$$\Delta S° = -(\Delta G° - \Delta H°) \,/\, T \quad \text{(S3)}$$

Where R and T are gas constant and absolute temperature respectively. Gibbs energy change was calculated in order to know if the extraction process was spontaneous or not.

3 Additional characterisation data for crude oil

The physical properties of crude oil vary significantly from one place to the other. The physical properties of the crude oil were determined using different methods and instruments, i.e., a tensiometer K9 was used to measure the surface tension, density (mass/volume), viscosity was measured using Alvatech QMC 922A, temperature (thermometer), pH (pH meter), API (American Petroleum Institute gravity (141.5-135/SG), water and sediment was measured using the centrifuge method which is known as the BS &W (Basic Sediment & water). A thermogravimetric analysis (TGA) of the crude oil was done to determine the water content of the crude before and after treatment with deep eutectic solvents.

Table S1 below summarises some of the properties of crude oil from Samabiri/Biseni flow station in Nigeria. The differences in the various properties of crude oil makes the refiners and the operation industries to boost their operation by selecting the best crude oil to meet the marketing needs.

Table S1 General properties of the crude oil obtained from Samabiri/Biseni flow station Bayelsa State, Nigeria.

Property	**Value**
Surface tension (mN/m) *	29.7
Density (g/cm^3) *	0.917
Viscosity (cP) *	128.66
API gravity	22.81
Specific gravity	0.917
Refractive index	1.66
Water and sediment (vol. %)	< 1%

*Average of three determinations at 23 °C.

As shown in **Table S1**, the API gravity of the crude oil is 22.81 which classifies it as heavy crude. The viscosity is as shown in the table is high compared to crude oil from the Basrah and Khanaken areas in Iraq.[7] crude oils with API gravity of less than 10.0 are classified as extra heavy crude, those of API gravity less than 22.3 are classified as heavy crude while those of API gravity of higher than 31.2 are classified as light crude.[8] The API and the viscosity of crude oil are very important parameters in the classification of crude. Crude oil viscosity can range from very low viscous liquid to up to high, tar-like near solid form.[7] Another very important parameter to determine the quality of crude oil is the density. From **Table S1**, the density of the crude oil at 23 °C is 0.917 g cm^{-3}. This is very close to that found in the Punjab-Pakistan area and the Basrah and Khanaken area of Iraq.[7]

In this study, the water content in Samabiri/Biseni crude oil was less than 1% compared with that of Iraq. This may the attributed to the topography of the Niger Delta area of Nigeria which is a rain forest with a flat foot delta below sea level.

3.1 UV-Vis spectroscopy

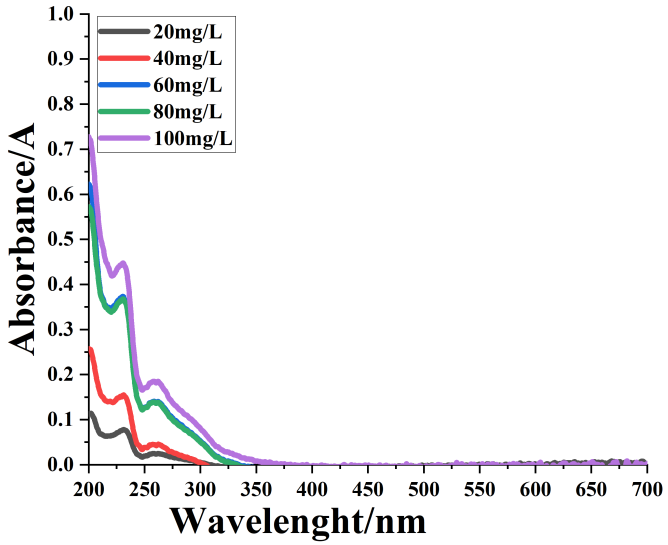

Figure S9 UV-Vis spectra of crude oil in cyclohexane, with a concentration range of 20 to 100 mg L^{-1} for Samabiri/Biseni crude oil.

Analysis of crude oil in cyclohexane was carried out using UV-Vis spectroscopy. It can be seen from the spectra in **Figure S9** above that, the absorption pattern was the same in all concentrations. Around 230 nm, there is an absorbance which corresponds to conjugated aromatic compounds like pyridine. There is another absorbance at 260–270 nm which correspond to naphthenic compounds. Finally, from 320–410 nm, and 600–700 nm, there are some very faint Soret and Q bands, indicating the presence of metal porphyrins. It is also clear from **Figure S9** that as the oil concentration in the solution decreases, the intensity of absorption decreases as effect of concentration.

3.2 FT-IR spectroscopy

FT-IR can be used to analyse and identify functional groups in crude oil.

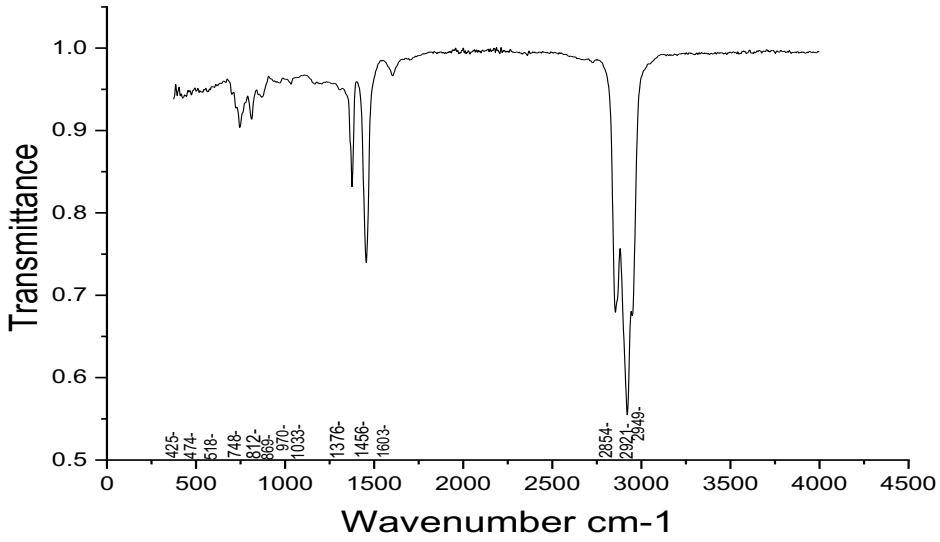

Figure S10 FT-IR spectrum for Samabiri/Biseni crude oil Bayelsa State, Nigeria.

It can be seen from **Figure S10** above that there is the presence of aromatic rings, anhydrides, aldehyde and ketone, phenyl rings, and alkanes. The stretching band appears at the frequency of 2949 cm^{-1}, and this is a clear indication of the stretching of CH-Ph which is benzylic moiety. Within the range of 2949–2921 cm^{-1}, symmetric and the asymmetric methyl (CH_3) stretching is observed. Furthermore, in the range of 2949–2854 cm^{-1}, the absorption bands for methylene (asym-CH_2 sym-CH_2) appear. A critical look at the spectrum shows that two bands appeared at 1456 and 1376 cm^{-1}. This can be attributed to the bonding of C-H. Bands which appear at frequencies of 1376 and 1456 cm^{-1} can be attributed to the presence of rotational vibration of CH_3 and CH_2 groups. Out of plane (=CH) stretching can be observed at frequencies of 748, 812 and 869 cm^{-1} respectively. The weak band at 1603 cm^{-1} can be attributed to C=C aromatic rings. All of these absorbance bans are typical of what would be expected for a crude oil sample.

3.3 Thermogravimetric analysis (TGA) and differential scanning calorimetry (DSC)

Figure S11 shows a thermogravimetric analysis/differential scanning calorimetry of the crude oil. The graph of the thermogravimetric analysis shows there is little or no water in the crude oil before and after extraction. It is non-isothermal thermogravimetry and differential thermal analysis (TGA-DTA). The analysis clearly identifies two main regions. This first region is the reaction between 140 and 450 °C which is known as low temperature oxidation (LTO).

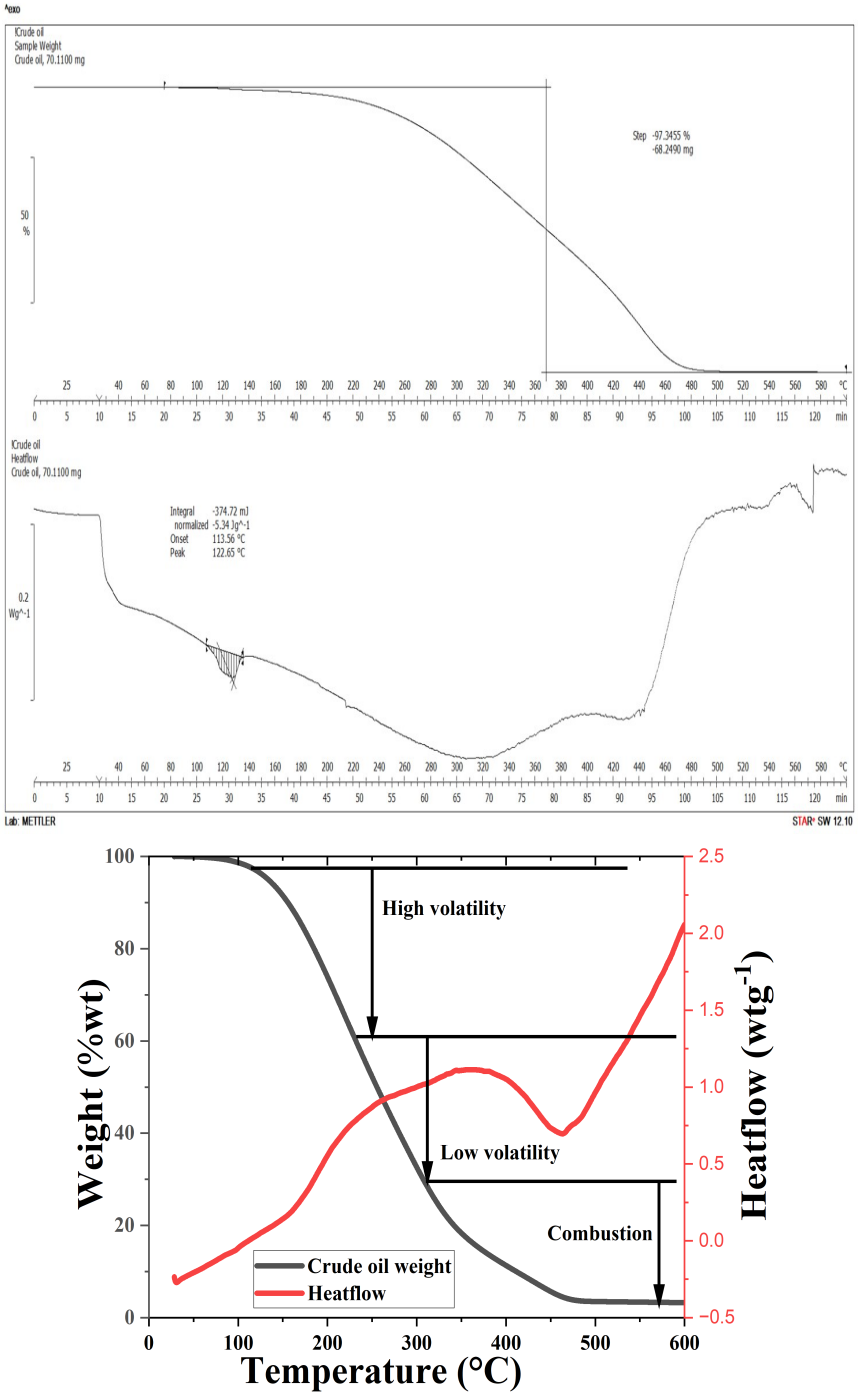

Figure S11 Graph of thermogravimetric analysis of crude oil under nitrogen (N_2).

This region is characterised by the low peak temperatures and also low levels of carbon oxides in the effluent gas stream. Another reaction was identified between 450–600 °C

and it is a cause of most of the exothermic heat of reaction with high temperature oxidation (HTO). A critical look at the graph shows that, major mass loss of the crude oil occurred in LTO region. Kok *et al.* (2016) reported that 70–90 % of mass loss in crude oil is in the (LTO) region which is the hydrocarbon of low molar mass while 10–30% of mass loss is in (HTO) and it is referred to as the degradation of hydrocarbon of medium molar mass.[9] Also, the heavy crude oil, the mass loss was highest in LTO region and lowest in HTO, as expected but in all, it depends on the API of the crude oil. The result is also similar to research by Kok *et al.* (2020), on low-temperature oxidation reactions of crude oils using TGA–DSC techniques.[10]

3.4 Inductively coupled plasma mass spectrometry (ICP-MS)

Three methods were applied for the ICP-MS analysis to know the actual concentration of metals in the crude oil before extraction. In the first method, approx. 0.07 g of crude oil was digested in 1 mL 70% trace metal grade HNO_3 and 2 mL 50% trace metal grade HF, heated in a sealed container, overnight, at 120 °C, sonicated for 30 min. Sample was dried down and retaken up in 3 mL of Trace Metal Grade HCl, heated in a sealed container, overnight, at 120 °C, sonicated for 30 min. This process was repeated again. Then, sample was dried down and retaken up in 4 mL of trace metal grade HCl, heated in a sealed container overnight, at 120 °C, sonicated for 30 min. Again, sample was dried down and retaken up in 3 mL of trace metal grade HNO_3 and a splash of DI water. The sample solution looked clear at this point, although the inside of the digest vessel still had obvious, undissolved, oil residue stuck to it. Sample was washed out with DI water into a pre-leached sample bottle and made up to approx. 100 g on the analytical balance (final precise weight was recorded) Sample is now ready for analysis. Although, precautionary measure of centrifuging to remove any undissolved suspended solids that may have been present was taken.
In the second method, approx. 0.07–0.1 g of crude oil was digested in 3 mL 70% trace metal grade HNO_3 and 1 mL 30% trace metal grade H_2O_2, heated in a sealed container for 1 hour at 120 °C and added extra H_2O_2 after the initial digest and then left on the hotplate for an extra hour. Sample was washed out into a 15 mL centrifuge tube with 10 mL of DI water. The sample solution was not clear and still had obvious suspended solids that remained undissolved. The inside of the digest vessel also still had obvious, undissolved; oil residue stuck to it. Sample was centrifuged at 5000 rpm for 10 min to remove suspended solids. A 1 mL aliquot was taken and diluted with 6.5 mL DI water (sample is now approx. 2% HNO_3 and ready for analysis)
The third method for the analysis of metal concentration in the crude oil, extraction induced by emulsion breaking (EIEB) was carried out according to de Sousa *et al.* (2019).[11] To do this, 0.5 g of the untreated crude oil and crude oil treated with DESs, crystalline organic acids, and botanical adsorbents was mixed with 2.5 mL of paraffin-wax (mineral oil) to modify the viscosity of the crude oil. Then 3 mL of an extractant solution which is made up of 20% (m/v) Triton X-114 and 6.5 mol dm^{-3} HNO_3 were added to the crude oil mixture. To achieve emulsification, the mixture was vigorously shaken. The emulsions were broken down by heating it at 90 °C for 40 min, it was then centrifuged at 5000 rpm for 15 min and at the end of centrifugation, two separate phases were clearly seen. After a thorough comparation of the three methods, using the third method was preferable as it was not time consuming, simple, quick and less cheap. It was also observed that, the third method was able to extract large quantity of the trace metals of interest for the ICP-MS analysis than the other two methods. As shown in **Table S2**, Mg, V, Fe, Ni, and Cu were determined by ICP-MS in the crude oil from

Samabiri/Biseni flow station using three different procedures. The results obtained using the first procedure as shown in **Table S2** shows a high concentration of V, Fe and Ni while Mg and Cu are below level of detection. A critical look at the second procedure as shown in **Table S2** indicates a high concentration of all the metals except for V which is low. This may be due to the contact of the crude oil with the salt water and other rocks in the area it was taken. From the results obtained as seen in **Table S2**, it is clear that the third procedure gives data which are more characteristic of this region, and this technique will be used in subsequent ICP-MS analysis.

Table S2 ICP-MS analysis of metal in crude oil using full digestion procedure with HNO_3, HF, and HCl.

Digestion method	**Metal concentration (ppb)**				
	Mg	**V**	**Fe**	**Ni**	**Cu**
HNO_3, HF, and HCl	<lod	1122.63	886.53	6553.17	<lod
HNO_3, and H_2O_2	1041.73	701.07	1886.61	6293.45	<1750
Extraction induced by emulsion breaking	13307	972	104340	10116	2914

These results are likely to have implication in the process of refining and also create environmental pollution issues. As an indicator to the maturity of crude oil, some researchers use the ratio of V/Ni while some think the ratio decreases as the producing field gets old, others are of the impression it increases.[11] The two elements, V and Ni are attached to porphyrins or in very rare cases to non-porphyrins complexes and anion of organic acids. The availability of V, Fe and Ni in crude oil can be used as an indicator of the organic matter in source of the crude oil. Studies have shown that oils obtained from sapropel type of organic matter (those with a high fatty acid and waxy hydrocarbon content but a low cellulosic content) have high V and Ni at a high ratio of V/Ni. While the humic types (with a high cellulosic content) has a low V and Ni at a high Fe content and low ratio of V/Ni. This probably originates from the ability of fatty acid compounds to form insoluble iron complexes.

3.5 DES-to-oil ratio and preliminary recyclability studies

Although experiments conducted using equal volumes of DES and crude oil provided effective extraction, a 1:1 v/v ratio was not deemed practical for large-scale application. Therefore, the effect of varying the DES-to-oil w/w ratio was investigated. **Figure S12** shows extractions performed using 1 g, 2 g, and 5 g of Ethaline with 10 g of crude oil, and 1 g, 2 g, and 5 g of Oxaline with 10 g of crude oil.

Recovery of the DES phase after extraction proved difficult when using 1 g or 2 g due to the small phase volume. Consequently, further experiments were conducted using 5 g of DES with 10 g of crude oil, and the solvent was reused for five consecutive extraction cycles.

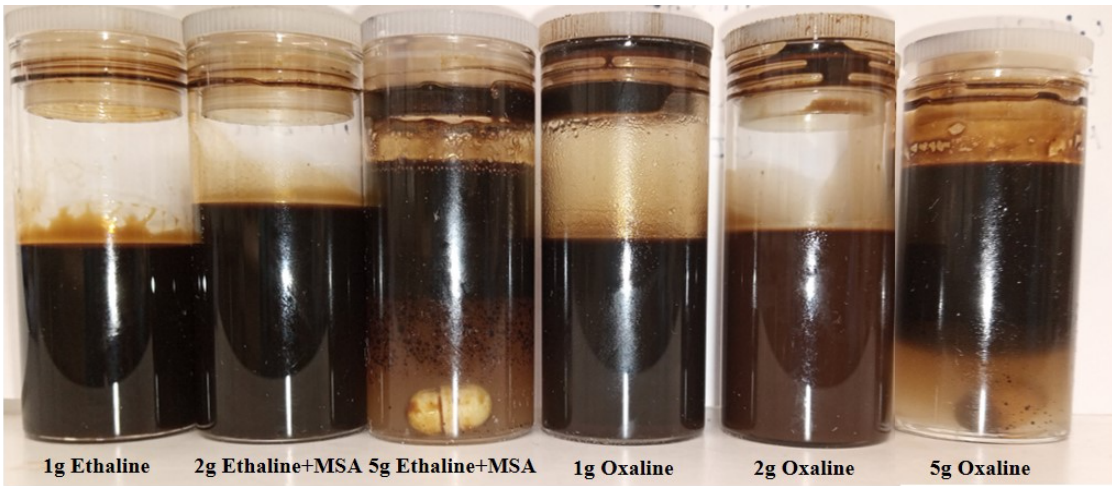

Figure S12 Crude oil treated with DESs at a w/w ratio of 10:1, 10:2, and 10:5.

To evaluate whether the DES becomes saturated with metal ions upon reuse, repeated extraction experiments were performed using Ethaline + MSA and Oxaline. As shown in **Figures S13** and **S14**, the percentage metal extraction remained essentially unchanged over five successive cycles. This indicates that the DES did not become saturated with metal ions under the experimental conditions.

Based on these results, the optimum operating conditions for metal extraction from crude oil using DESs were determined to be: extraction temperature 25 °C, contact time 40 min, DES-to-oil w/w ratio 1:1, and stirring rate 500 rpm.

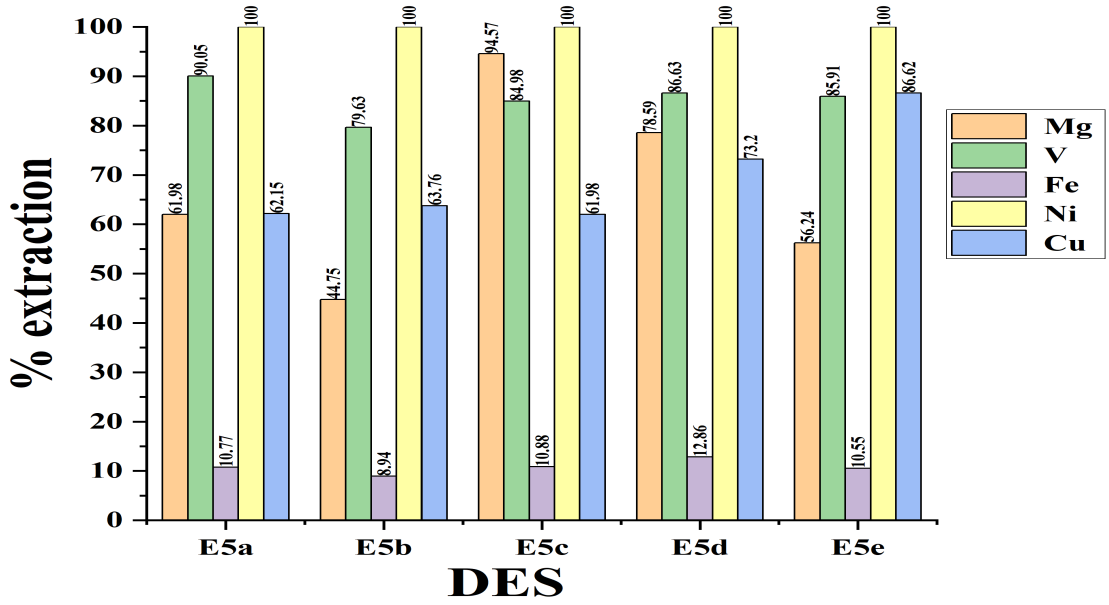

Figure S13 Effect of repeated reuse of the DES (Ethaline + MSA) on metal extraction from crude oil. Conditions: stirring rate 500 rpm, extraction time 40 min, temperature 25 °C, DES-to-oil w/w ratio 1:2.

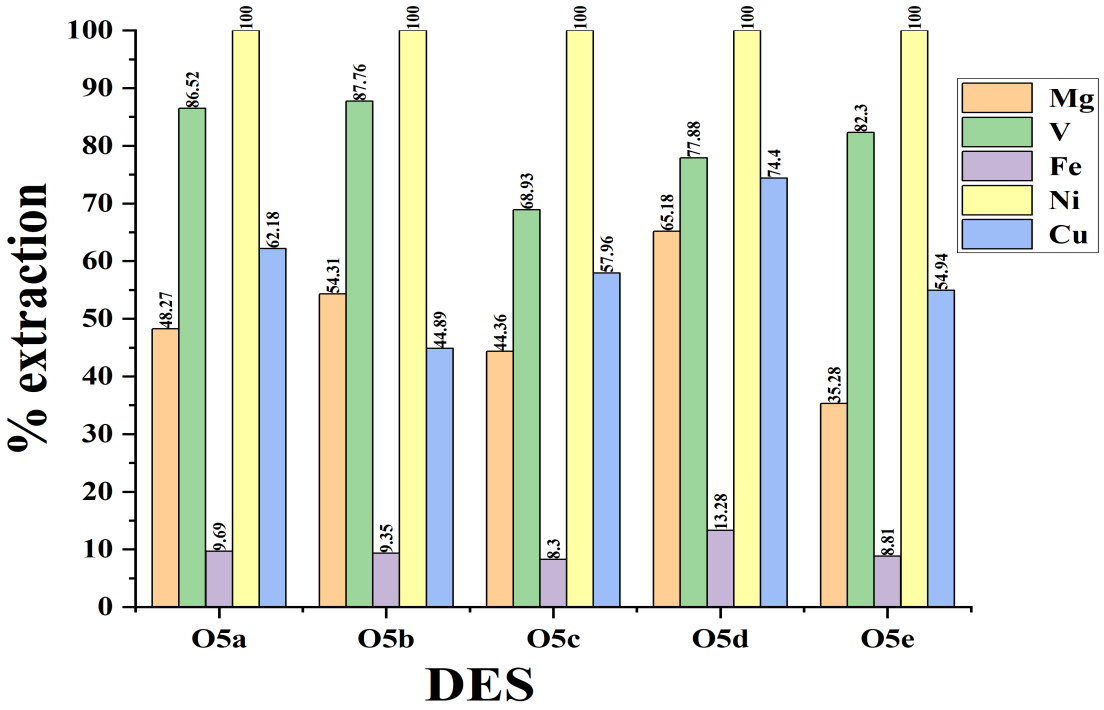

Figure S14 Effect of repeated reuse of the DES (Oxaline) on metal extraction from crude oil. Conditions: stirring rate 500 rpm, extraction time 40 min, temperature 25 °C, DES-to-oil w/w ratio 1:2.

Table S3 ICP-MS analysis of metal concentration in crude oil after repeated extraction with DES (Ethaline + MSA) using EIEB procedure.

	Mg	**V**	**Fe**	**Ni**	**Cu**
E1$_a$	5695	746	9816	11674	2729
E2$_a$	5290	880	10714	10787	1780
E5$_a$	8248	953	11240	13015	1811
E5$_b$	5955	774	9326	10730	1858
E5$_c$	12585	826	11347	11810	1806
E5$_d$	10458	842	13417	12528	2133
E5$_e$	7484	835	11007	12959	2524

E1 = 1 g of Ethaline, E 2= 2 g of Ethaline, E5 = 5 g of Ethaline.

Table S4 ICP-MS analysis of metal concentration in crude oil after repeated extraction with DES (Oxaline) using EIEB procedure.

	Mg	**V**	**Fe**	**Ni**	**Cu**
O1$_a$	6195	910	7820	10913	1459
O2$_a$	18527	697	11493	11764	1889
O5$_a$	6423	841	10114	13234	1812
O5$_b$	7228	853	9754	12293	1308
O5$_c$	5904	670	8658	11607	1689
O5$_d$	8674	754	13857	13655	2168
O5$_e$	4695	800	9191	13472	1601

O1 = 1 g Oxaline, O2 = 2 g Oxaline, O5 = 5 g Oxaline.

3.6 Methodology for approximate costs of acids for metal extraction using DESs

The price of the raw acids was obtained as a range https://www.alibaba.com accessed in August 2024. Prices are provided as a range depending on supplier, volume ordered and product purity. In principle the acid is used up in the process as the metal will be precipitated as a salt with the anion of the acid so the extraction does not, in principle, use up the salt of the DES. We have factored in a 10% mechanical loss of DES with each run. The energy costs for stirring were ignored in this calculation as they were small in comparison to the chemical costs.

4 Additional references

1 R. K. Sharma, C. Sharma and I. T. Sidhwani, *J. Chem. Educ.*, 2011, **88**, 86–87.
2 J. M. Hartley, C.-M. Ip, G. C. H. Forrest, K. Singh, S. J. Gurman, K. S. Ryder, A. P. Abbott and G. Frisch, *Inorg. Chem.*, 2014, **53**, 6280–6288.
3 A. P. Abbott, A. Y. M. Al-Murshedi, O. A. O. Alshammari, R. C. Harris, J. H. Kareem, I. B. Qader and K. Ryder, *Fluid Phase Equilib.*, 2017, **448**, 99–104.
4 A. T. Davidson, *J. Chem. Phys.*, 1982, **77**, 168–172.
5 M. Attia, S. Farag, S. A. Jaffer and J. Chaouki, *J. Clean. Prod.*, 2020, **275**, 124177.
6 M. M. El-Nahass, Z. El-Gohary and H. S. Soliman, *Opt. Laser Technol.*, 2003, **35**, 523–531.
7 A. K.-T. Mohammad, A. T. Hameed, M. A. Alhamdany, K. Mohammad Al Azzam and G. A. A. Talk, *Biomed. Chromatogr.*, 2019, **33**, e4481.
8 R. E. C. Pabón and C. R. de Souza Filho, *Fuel*, 2019, **237**, 1119–1131.
9 M. V. Kök, M. A. Varfolomeev and D. K. Nurgaliev, *J. Pet. Sci. Eng.*, 2017, **154**, 537–542.
10 M. V. Kok, M. A. Varfolomeev and D. K. Nurgaliev, *J. Therm. Anal. Calorim.*
11 J. M. de Sousa, R. J. Cassella and F. G. Lepri, *Energy & Fuels*, 2019, **33**, 10435–10441.